Adhesion of metal–carbide/nitride interfaces: Al/TiC and Al/TiN

2003 J. Phys.: Condens. Matter 15 8103

(http://iopscience.iop.org/0953-8984/15/47/013)

INSTITUTE OF PHYSICS PUBLISHING JOURNAL OF PHYSICS: CONDENSED MATTER

J. Phys.: Condens. Matter **15** (2003) 8103–8114 PII: S0953-8984(03)68073-2

Adhesion of metal–carbide/nitride interfaces: Al/TiC and Al/TiN

L M Liu[1], **S Q Wang and H Q Ye**

Shenyang National Laboratory for Materials Science, Institute of Metal Research, Chinese Academy of Sciences, Shenyang 110016, People's Republic of China

E-mail: lmliu@imr.ac.cn

Received 27 August 2003, in final form 24 September 2003
Published 14 November 2003
Online at stacks.iop.org/JPhysCM/15/8103

Abstract

We employ density functional theory to investigate and compare Al/TiC and Al/TiN interfaces by electronic structures, relaxed atomic geometries and adhesions. The results show that the preferred bonding site is the interfacial Al atoms above the ceramic's metalloid atoms for both systems. The calculated adhesion energies are quantitatively in agreement with other calculated and experimental results of Al on the carbide and nitride. A detailed comparison of the adhesion energies and relaxed structures shows weaker bonding and less relaxation in the Al/nitride case, which is correlated with the lower surface energy of the ceramic. We have thoroughly characterized the electronic structure and determined that the polar covalent Al3sp–C(N)2s bonds constitute the primary interfacial bonding interaction. The larger overlapping bonding states at the Al/TiC interface reveal the reason why it exhibits relatively larger adhesion energy. Cleavage may take place preferentially at the interface, especially for the Al/TiN, which is in agreement with experimental results.

1. Introduction

Many transition metal carbides and nitrides not only have the NaCl structure, a typical feature of ionic crystals, but also high melting points and hardness, characteristics of covalent compounds. They present an unusual combination of physical, chemical, and mechanical properties, which make them highly attractive from a technological as well as the fundamental point of view [1, 2].

Titanium carbide and nitride, due to having such excellent properties, are commonly used in wear- or corrosion-resistant coatings and mechanical components, electrical contacts, diffusion barriers in electronic devices, and metal matrix composites [3–5]. The structural strength for such materials can depend on the adhesion of the metal–ceramic interfaces, so the interfaces between the ceramic and the substrate metal or matrix are rather important. To optimize the properties of these materials it is important to have a good understanding of the

[1] Author to whom any correspondence should be addressed.

0953-8984/03/478103+12$30.00

internal heterointerfaces. Both the formation process and the performance of these materials are, to a large extent, affected by the interfaces between the metal and the ceramic.

Many first-principle density functional theory (DFT) calculations have been applied to metal–ceramic interfaces, but most of them [6–16] are confined to metal–oxide interfaces. Recently, metal–transition metal carbide or nitride interfaces have been studied [17–21], but they are not widely explored theoretically. Unlike the ceramic oxides, most of the carbides and nitrides are conducting, and their bonding characteristics are considered to be a mixture between covalent and ionic. Thus the mechanism of metal–carbides or nitrides may differ essentially from the case of the metal–oxides. Dudiy and Lundqvist [18] studied Co/TiC(N)(001) interfaces. Their results showed that the dominant bonding of the interface was a strong covalent bond between the Co-3d and C(N)-2p orbital, and the calculated adhesion strength was consistent with the wetting experiments. Siegel and co-workers [19] calculated the polar Al/WC(0001) interface, and found the optimal C-terminated structure, which formed the polar covalent bonds, was nearly 2 J m^{-2} stronger than that of W-terminated.

On the experimental side, several groups, due to the industrial importance of such materials, have widely fabricated and investigated the Al/TiC or Al/TiN interfaces. The interfacial reaction, the wetting, and the fracture have been examined [5, 22–28]. However, the factors which determine the adhesive and electronic properties of the interfaces are still poorly understood. The evaluation of such coatings or composite is often poorly performed on a traditional trial-and-error basis. So, the understanding of metal–carbide/nitride bonding at the atomic level, a very valid goal for fundamental science, could stimulate ideas for optimizing the performance of these interfaces.

The purpose of this work is to calculate the electronic structures, adhesion energies and optimal geometries of several representative Al/TiC and Al/TiN interfaces, within the framework of DFT in order to shed some light upon the correlation between the work of adhesion and the atomic or electronic structures of metal–ceramic. Meanwhile, it also compares the Al/TiC interface to the Al/TiN case and in this way provides microscopic level insight into the fundamental differences between them.

The remainder of this paper is organized as follows. Section 2 describes the computational methodology used in this study. Section 3 presents the results of our bulk and surface calculations on the pure and compound materials. The major results of this paper are presented in section 4, where we discuss and compare the two systems' properties of interfacial adhesion energies, electronic structures, and fractures. Finally, we summarize our results in section 5.

2. Methodology

We utilize the dacapo [29] package in our calculations, based on DFT [30, 31], which uses a plane-wave (PW) basis set for the expansion of the single-particle Kohn–Sham wavefunctions and Vanderbilt ultrasoft pseudopotentials (USPP) [32] to describe ionic cores. The exchange–correlation energy is described by the generalized gradient approximation of Perdew and Wang (GGA-PW91) [33]. The self-consistent PW91 density is determined by iterative diagonalization of the Kohn–Sham Hamiltonian, coupled with a Pulay mixing scheme [34]. A Fermi function is used with a temperature broadening parameter of 0.2 eV to improve the convergence. Ground-state atomic geometries are determined by minimizing the Hellman–Feynman forces, and the dipole correction [35] perpendicular to the interface is added. The Brillouin zone is sampled with a Monkhorst–Pack k-point grid [36]. For the bulk a [$8 \times 8 \times 8$] k-point mesh is used and for the slab a [$8 \times 8 \times 1$] k-point mesh is used. The PW cut-off in our calculations is 350 eV. This set of parameters assures a total energy convergence of 0.01 eV/atom.

Table 1. Calculations of the lattice constant (a_0), bulk module (B), and cohesive energy (E_{coh}) of the bulk Al, TiC and TiN compared with other calculated and experimental (Expt) data.

System	Method	a_0 (Å)	B (Mbar)	E_{coh} (eV)
TiC	This work	4.33	2.48	7.2
	GGA-PWPP[a]	4.33	2.52	7.3
	GGA-FP-LMTO[b]	4.315	2.2	—
	Expt	4.33[c]	2.42[d]	7.04[d]
TiN	This work	4.25	2.78	6.80
	GGA-PWPP[e]	4.236	2.82	—
	GGA-FP-LMTO[b]	4.23	2.7	—
	Expt	4.238[f]	2.88[g]	6.69[h]
Al	This work	4.05	0.75	3.45
	GGA-PWPP[i]	4.039	0.735	3.54
	GGA-LAPW[j]	4.05	0.73	—
	Expt[k]	4.05	0.72	3.39

[a] Reference [18].
[b] Reference [38].
[c] Reference [39].
[d] Reference [1].
[e] Reference [40].
[f] Reference [41].
[g] Reference [42].
[h] Quoted in Reference [43].
[i] Reference [14].
[j] Reference [44].
[k] Reference [45].

3. Bulk and surface calculations

3.1. Bulk properties

To assess the accuracy of our computational method, in particular of the pseudopotentials used, we performed a series of calculations on the bulk properties of Al, TiC, and TiN. The ground state lattice constant, bulk modulus and bulk total energy were determined via a fit of energy volume data to Murnaghan's equation of state [37]. Table 1 compares our results for the lattice constants, bulk modulus, and cohesive energies with those of other calculations and experiments.

We note that all our calculated results of lattice constant are in good agreement with the experimental results. For TiC, the cohesive energy, 7.2 eV, agrees with the experimental value [1] to within 3%. The bulk modulus of 2.48 Mbar is only overestimated by 2% compared with the experimental value [1]. For TiN, the bulk modulus, 2.78 Mbar, is underestimated within 4% of the experimental value [42], and overestimated with respect to the other full-potential linear-muffin-tin-orbital (FP-LMTO) value [38]. For Al, the cohesive energy and bulk modulus agree well with the experimental results [45].

3.2. Surface properties

It is important to make sure that both side of the slabs are thick enough to show the bulk-like characteristic interiors, as it is known that the adhesion properties of thin films can differ significantly from those of thicker ones. So, we first do some convergence tests on the Al(001), TiC(001) and TiN(001) slabs with respect to slab thickness.

Table 2. The convergence of the surface energy with respect to slab thickness.

	Surface energy (J m^{-2})		
Layers, n	Al(001)	TiC(001)	TiN(001)
3	0.88	1.67	1.32
5	0.91	1.65	1.28
7	0.95	1.64	1.27
9	0.95	1.64	1.27
11	0.94	1.64	1.27

One way to ensure the presence of a bulk-like slab is to check for the convergence of the surface energy with respect to the number of atomic layers, n. Upon attaining a critical thickness, the surface energy will converge to a fixed value, indicating that the two surfaces are decoupled by an interior bulk region. We have calculated the surface energy for each (001) face of Al, TiC and TiN for slabs of thickness ranging from 3 to 11 layers using the method proposed by Boettger [46, 47]. In order to prevent the interactions between the slab and its periodic images, a vacuum region of at least 10 Å is included in the supercell [48, 49]. All structures are relaxed to a force tolerance of 0.05 eV Å^{-1}.

As is shown in table 2, the surface energy for all materials converges rapidly with increasing slab thickness to within about 0.04 J m^{-2} for slabs with $n \geqslant 5$. For Al, our calculated surface energy for the 5-layer slab (0.91 J m^{-2}) is consistent with the other calculated value of 0.89 J m^{-2} [20]. We further note that the present value of the Al(001) surface energy is in good agreement with the experimental values of 0.948 J m^{-2}, as extrapolated to 0 K [50]. For TiC and TiN, the calculated values of 1.64 and 1.27 J m^{-2} (7-layer) are in agreement with other GGA-DFT results of 1.665 J m^{-2} for TiC [51] and 1.30 J m^{-2} for TiN [40], respectively.

In addition to our examination of the surface energy, we consider the surface relaxations as a function of slab thickness. We find that these are also well converged by 5–7 layer slabs, with all relaxations being a relatively small amount (2% or less) of the corresponding bulk spacings. For Al(001) the first interlayer spacing increases by 2%, which is consistent with the result of [20]. For TiC the first interlayer spacing contracts by 1.5%. The obtained relaxation of the TiC(100) surface is Ti 0.074 Å inward and C 0.041 Å outward, and this gives a surface rippling, i.e., a difference in C and Ti displacements, of $r = 0.115$ Å. This is in good agreement with the other calculated result, $r = 0.14$ Å [52] and experimental result, $r = 0.13$ Å [53]. For TiN the first interlayer spacing contracts by 1.1%. The surface has the same direction of relaxation as TiC, but the magnitude is a little larger, Ti 0.098 Å inward and N 0.058 Å outward. So the rippling of the TiN surface is 0.156 Å, which is larger than that of TiC.

In conclusion, we have shown that our calculated values of the bulk and surface properties for Al, TiC and TiN are in good agreement with available experimental and other calculated results, thereby validating the application of the methodology to study the interfacial properties.

4. Interfaces

4.1. Model geometry

Our model of the Al/TiC and Al/TiN interfaces uses a superlattice geometry in which a 5-layer slab of Al(001) is placed on a 7-layer TiC or TiN(001) slab. The free surfaces of Al and TiC or TiN are separated by at least 10 Å vacuum. In addition to interfacing the (001) planes,

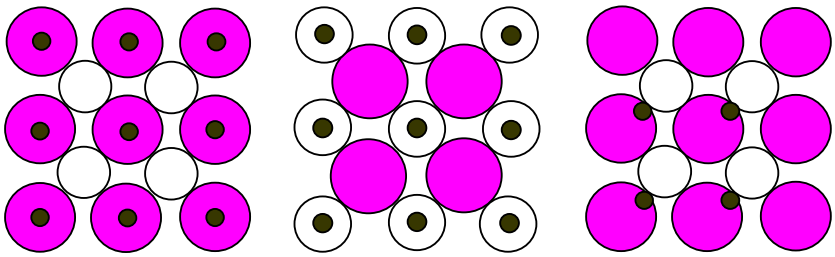

(a) Ti-site (b) C/N-site (c) Bridge-site

Figure 1. Three stacking sequences for the Al/TiC or Al/TiN interfaces. The small spheres represent the Al atoms; the medium-sized spheres represent the C/N atoms; the large spheres represent the Ti atoms.

(This figure is in colour only in the electronic version)

the slabs are oriented about an axis normal to the interface so as to align the [001] directions, resulting in a 'cube-on-cube' orientation relationship [20]:

$$\mathrm{Al}[001](001) \parallel \mathrm{TiC/TiN}[001](001).$$

Using this orientation, there is a modest lattice mismatch of 6.7% (4.8%) between the larger TiC (TiN) and the Al. To accommodate the periodic boundary conditions inherent in a supercell calculation, we invoke the coherent interface approximation [54] in which the softer Al is to match the dimensions of the TiC or TiN.

To identify the optimal interface geometry we consider three different stacking sequences, placing the interfacial Al in one of three positions with respect to the ceramic surface lattice structure, as shown in figure 1: Al above the C/N atoms (C/N-site), Al above the Ti atoms (Ti-site), and along the Ti–C/N bond direction (bridge-site). Adhesion energies are then calculated for all geometries after allowing for the atomic relaxations.

4.2. Interface structure, work of adhesion

The ideal work of adhesion, W_{ad}, an important fundamental quantity to predict the mechanical properties, is defined as the reversible work needed to separate an interface into two free surfaces. W_{ad} can be given by the difference in total energy between the interface and its isolated slabs:

$$W_{\mathrm{ad}} = (E_{\mathrm{A}}^{\mathrm{tot}} + E_{\mathrm{B}}^{\mathrm{tot}} - E_{\mathrm{A/B}}^{\mathrm{tot}})/A. \tag{1}$$

Here, $E_{\mathrm{A}}^{\mathrm{tot}}$ and $E_{\mathrm{B}}^{\mathrm{tot}}$ are the total energy of the relaxed, isolated TiC or TiN and Al slabs in the same supercell when one of the slabs is kept and the other one is replaced by vacuum, respectively, and $E_{\mathrm{A/B}}^{\mathrm{tot}}$ is the total energy of the Al/TiC or Al/TiN interface system. A is the total Al/TiC or Al/TiN interface area of the unit cell. Generally, the mechanical work needed to separate an interface is larger than the ideal work of adhesion, W_{ad}, due to neglecting plastic and diffusional degrees of freedom, as discussed by Finnis [6]. Meanwhile the strain applied to the interface model, due to the lattice mismatch, will also play a significant role in biasing the calculated value [55, 56].

The interface geometries and the isolated slabs are optimized via minimization of the atomic forces to a tolerance of 0.05 eV $\mathrm{Å}^{-1}$. For the Ti- or C/N-site, all atomic relaxations are along the direction perpendicular to the interface due to the symmetry, and all in-plane

Table 3. Calculated relaxed work of adhesion (W_{ad}) and the interfacial separation (d_0) for the three Al/TiC and Al/TiN interface systems.

System	Stacking	d_0 (Å)	W_{ad} (J m^{-2})
TiC	Ti-site	2.70	0.51
	Bridge-site	2.29	1.44
	C-site	2.08	2.63
	Al Cleave		1.92
	TiC Cleave		4.03
TiN	Ti-site	2.76	0.39
	Bridge-site	2.54	0.50
	N-site	2.09	1.39
	Al Cleave		1.57
	TiN Cleave		3.29

forces are equal to zero. The structure of the bridge-site is constrained to allow relaxation perpendicular to the interface only.

Our calculated results of the optimal interfacial separation (d_0) and work of adhesion (W_{ad}) for all six interface structures are shown in table 3. The interfaces with the Al atoms placed above the metalloid atoms exhibit the largest W_{ad} value of 2.63 and 1.39 J m^{-2} for the Al/TiC and Al/TiN, respectively. The bonding over the Ti-site is weakest, and the bridge-site is between the two extremes. The preferred places and sequences of three sites are consistent with other metals on carbides, nitrides or even oxides [20, 55].

For the Al/TiC, the calculated W_{ad} of the C-site is a little higher than the result of recent wetting experimental results, 1.61 J m^{-2} [24]. It should be pointed out that the experimental result is for molten drops of metal on carbides, while our result is for a solid slab, which is substantially larger than for the molten drop as discussed in [57]. Meanwhile, misfit dislocations in the experimental sample, due to the lattice misfit between the Al and ceramic, will reduce the work of adhesion [6, 56]. For the Al/TiN, there is no available experimental result to compare with. The relatively low W_{ad} values are of the same order of magnitude as other results of aluminium on carbide and nitride (2.13, 1.73 J m^{-2}) [20]. Further, our W_{ad} values for both carbide and nitride are noticeably larger than that of aluminium on MgO (0.55 J m^{-2}), which is also the NaCl structure but more ionic [55].

We note that the TiC, having higher surface energy, has larger adhesion energies than the corresponding TiN. This is consistent with the wetting experiment, which shows that the wettability of titanium carbide is better than that of titanium nitride [3]. Our calculated W_{ad} of Al/TiC(TiN) is a little larger than that of Al/VC(VN) [20]. The reason may be that surface energy of bulk TiC(TiN), which is a more reactive surface, is a little higher than that of VC(VN) (the surface energies for VC and VN are 1.27 and 0.95 J m^{-2}, respectively). So interfacial adhesion for the same systems is in correlation with the corresponding surface energy. The higher the surface energy, the higher the adhesion energy. This is consistent with other studies for other carbide, nitride, and oxide systems [20, 55, 58]. But this relation is not suitable for VC and TiN, which belong to carbide and nitride systems, respectively. They have nearly the same surface energy, but the adhesion energy of VC is almost 0.74 J m^{-2} larger.

Some interesting features are also observed in the perpendicular relaxation of the interfacial TiC and TiN layers. For the Al/TiC, the interfacial Ti atoms have the same (inward) direction and the same order of magnitude of perpendicular relaxation as the free TiC(001) surface. The C atoms are nearly 0.14 Å further out than the Ti atoms and the rippling of interfacial Al and C atoms become more obvious. For the Al/TiN the Ti atoms go 0.063 Å outward and the N atoms

also go 0.010 Å outward, relative to the free TiN(001) surface. The rumpling of the interfacial TiN slab becomes 0.103 Å. The formation of the interface smoothes the original rippling of the free TiN surface by 0.053 Å. The interlayer distance of the Al/TiC is 2.08 Å, which is shorter than that of the Al/TiN (2.09 Å). The different relaxation and interlayer distance of the Al/TiC and Al/TiN are a result of the different strengths of Al–C and Al–N interactions, which will be discussed later.

One important feature common to strongly bound interfaces is that the failure of the metal–ceramic interface does not occur by interface separation, but instead, it fails in the softer bulk material as found in other strong interface systems [12, 19]. In essence, the formation of an interfacial bond weakens the bond around the interfacial material. The interfacial bond becomes stronger than that of the interfaced material. To explore the possibility for the Al/TiC and Al/TiN interfaces, we carried out additional C/N-site calculations. The interfaces are cleaved within the softer Al slab, leaving a monolayer of Al on the surface, or within the sub-interfacial layer of the ceramic. The results are listed as 'Al Cleave' and 'TiC(TiN) Cleave' in table 3, respectively.

It is obvious that the interface adhesion of the C/N-site is substantially lower than that of TiC(TiN) Cleave, so the fracture has possibly not happened within the ceramic layers. The cleave adhesion of Al Cleave is rather close to the interface adhesion, and especially for Al/TiN the interface adhesion is only 0.16 J m^{-2} larger than the corresponding Al Cleave adhesion. A subsequent electronic structure study showed that the interfacial Al–C/N bond is a strong directional covalent bond, which is brittle, while the soft substrate Al is a metallic bond, which has excellent ductility. Meanwhile, the strain energy, due to lattice mismatch, will also facilitate the interface de-adhesion [9]. So, for the Al/TiC, the Al slab probably undergoes some work hardening/plastic deformation first during tensile loading, then with the help of strain energy the failure point may happen at the interface, and for the Al/TiN the interface will fracture directly at the interface. A recent four-point bend experimental test, which shows that the Al/TiC first has some plastic deformation in the softer Al matrix, and then cracks propagate along the interface [22], confirms our prediction. For the Al/TiN, the fracture experiment also indicates that fracture happens at the interface and it has relatively lower fracture strength than the Al/TiC [22, 26], consistent with our results.

In summary, we find relatively small W_{ad} values and preferred places for both Al/TiC and Al/TiN interfaces, consistent with other studies of Al with carbide/nitride. We predict that the failure point may be at the interface, especially for the Al/TiN, which is consistent with experimental results.

4.3. Electronic structure and bonding

To better analyse the bonding nature of abrupt metal–ceramic interfaces, we have used difference charge density, planar-averaged charge density, and density of states (DOS) to study the interfacial electronic structure and bonding. The difference charge density $\Delta\rho$ is given by

$$\Delta\rho = \rho_{\text{interface}} - \rho_{\text{ceramic}} - \rho_{\text{Al}} \tag{2}$$

where $\rho_{\text{interface}}$ is the total charge density of the interface systems, and ρ_{ceramic} and ρ_{Al} are the isolated TiC (TiN) and Al slabs of the same supercell, respectively.

Figure 2 shows the difference charge density on (110) planes for the C/N-site of Al/TiC (TiN), respectively. The two systems share some common features. First, the interfacial charge redistribution is rather localized, being confined to within the first metal layer and second ceramic layer. Second, both structures have a large amount of charge accumulation along the Al–C/N bond, which is a roughly spherical hump. On the other hand, there are

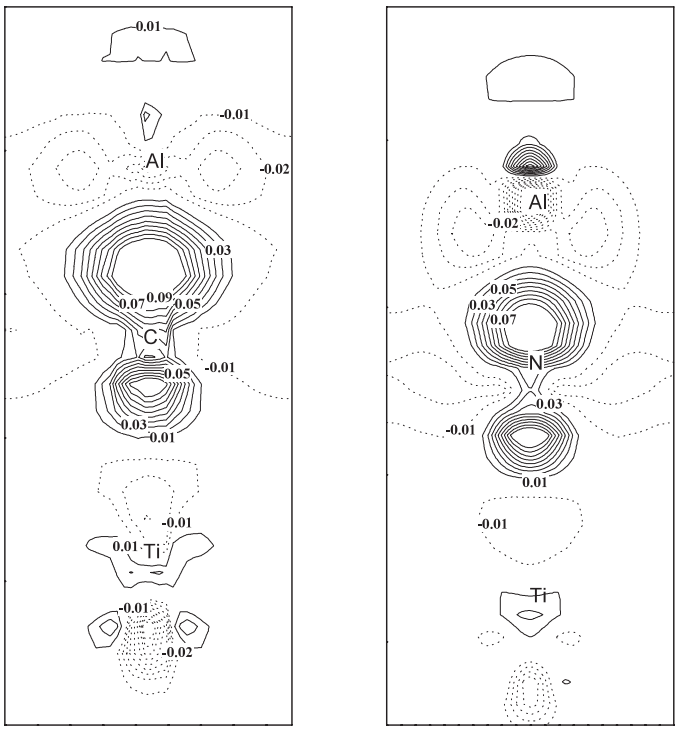

(a) Al/TiC (b) Al/TiN

Figure 2. Difference charge density for the Al/TiC (a) and Al/TiN (b) interfaces taken along the (110) plane. Contours range from -0.1 to 0.1 electron Å^{-3} and increase by 0.01 electron Å^{-3}. Solid (dashed) curves indicate positive (negative) values.

also some significant differences in the interfacial bonding characteristics of the Al/TiC and Al/TiN. First, the charge accumulation of Al/TiC is distinctly larger than that of Al/TiN. This is supported by the planar-averaged difference charge density as shown figure 3, which shows a remarkably larger peak at Al/TiC interface. Second, for Al/TiC the charge depletion is mainly along the lateral Al slab; for Al/TiN the charge depletion of the interfacial Al slab is rather localized and there is obviously charge depletion from the lateral TiN slab as shown in figures 2 and 3.

A more detailed picture of how the Al/TiC and Al/TiN interface bonds form can be extracted from the analysis of the layer-projected DOS as shown in figure 4. We note that both metal and ceramic slabs rapidly screen the effect of the interface, as the DOS beyond the interfacial layer has little difference from the corresponding bulk. This is consistent with the above results of charge distribution.

For Al/TiC the DOS of the interfacial Al layer shows a set of new low-energy states from -12 to -10 eV, which is an identically shaped feature to the DOS of the interface TiC. These new states make the TiC and Al larger overlapping states. The original peaks (-10 to -6 eV) of the interfacial Al slab, which just correspond to the energy band gap of TiC, have been weakened. Further, the DOS of the interfacial TiC layer also moves a little towards the low-energy states to overlap with that of interfacial Al. The interfacial TiC and Al slab form a common new DOS peak (about -11.5 eV).

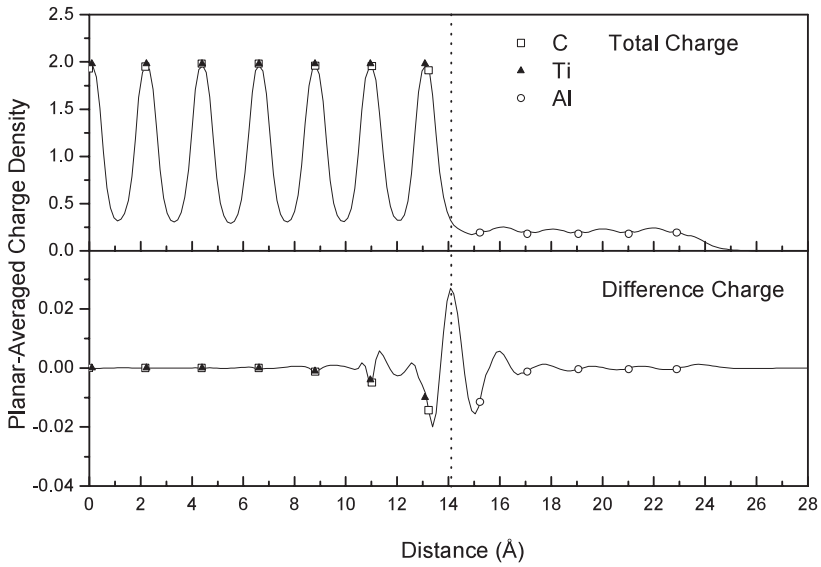

(a) Al/TiC

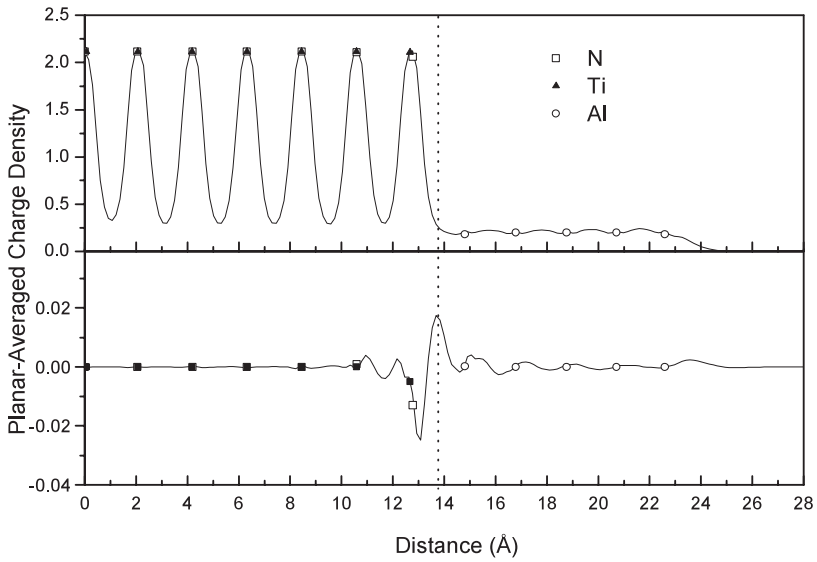

(b) Al/TiN

Figure 3. Planar-averaged total charge and difference charge density (relative to the isolated surfaces) for the Al/TiC (a) and Al/TiN (b) structures along a direction normal to the interfaces. The vertical dotted lines give the location of the interfaces.

For Al/TiN the DOS of the interfacial TiN layer has not obviously changed. For the interfacial Al slab, like Al/TiC, also shows a set of new states from −17 to −15 eV, corresponding to the states of N2s. Compared to TiC, TiN has one more electron per metal–nitride bond, which causes a shift of the N-sp and Ti-d states downward, away from the Al3sp states. This

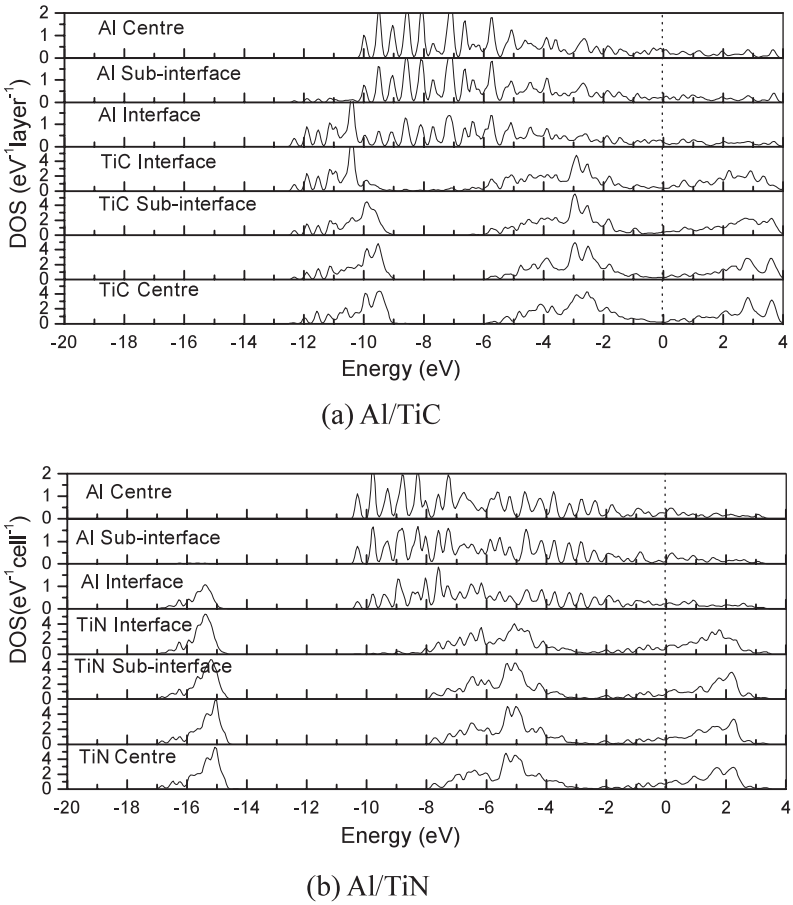

Figure 4. Layer-projected DOS for the Al/TiC (a) and Al/TiN (b) interface structure. The vertical dotted line gives the location of the Fermi level.

reduces the opportunity of Alsp–N2s interaction at the Al/TiN interface as shown in figure 4. This may be the reason why the strength of the Al–N bond is lower than that of the Al–C bond.

In all, the dominant interfacial bonding mechanism is strong Al3sp–C/N2s polar covalent interaction for both Al/TiC and Al/TiN. That the Al/TiC has relatively more overlapping states between the Al3sp–C2s at the interface is the reason why Al/TiC has larger adhesion energy.

5. Summary and conclusions

We have conducted a first-principles study of the adhesion, electronic structure, and bonding of Al/TiC and Al/TiN interfaces in order to understand the nature of the interface. We characterize the bulk and surface properties of Al, TiC and TiN, and our results are in good agreement with available experimental and other calculated results. For both carbide and nitride, we find that the preferred stacking sequence is Al atoms above the metallic C/N atoms, consistent with other studies of metal on other NaCl structures of carbide, nitride, and oxide. The calculated adhesion energies are quantitatively in agreement with available calculated and experimental results of Al on other carbide and nitride.

We have also clarified the differences in the interface interaction between the Al/TiC and Al/TiN interfaces. The interfacial adhesion energy is correlated with the ceramic surface energies for the carbide or nitride system. The adhesion increases linearly with surface energy. However, this relation is not suitable for VC and TiN, which belong to carbide and nitride systems, respectively. They have nearly the same surface energy, but the Al/VC shows obviously larger adhesion energy than Al/TiN.

To explore the essence of the different interfacial adhesion energies, we analyse and compare the electronic structures of both Al/TiC and Al/TiN using difference charge density, planar-averaged charge density and layer-projected DOS. The interfacial Al3sp–C/N2s interaction characterizes the polar covalent bond. The effects of the interface on the electronic structure of both the metal Al and the ceramic are mainly localized within the first and second layer. Compared with the Al–N bond, the Al–C case exhibits greater overlapping bonding states, explaining well its larger W_{ad}.

Finally, due to the directional covalent bond, strain energy, and relatively low adhesion energy, cleavage may take place preferentially at the interface, especially for Al/TiN. This is consistent with experimental results.

Acknowledgments

The authors are grateful to Dr Asbjorn Christensen for fruitful discussion and kind help. This work was supported by the Special Funds for Major State Basic Research Projects of China (No. G2000067104).

References

[1] Toth L E 1971 *Transition Metal Carbides and Nitrides* (New York: Academic)
[2] Joansson L I 1995 *Surf. Sci. Rep.* **21** 177
[3] Xiao P and Debry B 1996 *Acta Mater.* **44** 307
[4] Frumin N, Frage N, Polak M and Dariel M P 1997 *Scr. Mater.* **37** 1263
[5] Hultman L 2000 *Vacuum* **57** 1
[6] Finnis M W 1996 *J. Phys.: Condens. Matter* **8** 5811
[7] Batyrev I G, Alavi A and Finnis M W 2000 *Phys. Rev.* B **62** 4698
[8] Li C, Wu R, Freeman A J and Fu C L 1993 *Phys. Rev.* B **48** 8317
[9] Christensen A and Carter E A 2000 *Phys. Rev.* B **62** 16968
[10] Javis E A and Carter E A 2002 *J. Phys. Chem.* B **106** 7995
[11] Wang X G, Smith J R and Scheffler M 2002 *Phys. Rev.* B **66** 073411
[12] Wang X G, Smith J R and Evans A 2002 *Phys. Rev. Lett.* **89** 286102
[13] Zhang W and Smith J R 2000 *Phys. Rev. Lett.* **85** 3225
[14] Siegel D J, Hector L G Jr and Adams J B 2002 *Phys. Rev.* B **65** 085415
[15] Bogicevic A and Jennison D R 1999 *Phys. Rev. Lett.* **82** 799
[16] Zhukovskii Y F, Kotomin E A, Jacobs P W M and Stoneham A M 2000 *Phys. Rev. Lett.* **84** 1256
[17] Dudiy S V, Hartford J and Lundqvist B I 2000 *Phys. Rev. Lett.* **85** 1898
[18] Dudiy S V and Lundqvist B I 2001 *Phys. Rev.* B **64** 045403
[19] Siegel D J, Hector L G Jr and Adams J B 2002 *Surf. Sci.* **498** 321
[20] Siegel D J, Hector L G Jr and Adams J B 2002 *Acta Mater.* **50** 619
[21] Siegel D J, Hector L G Jr and Adams J B 2003 *Phys. Rev.* B **67** 092105
[22] Katipelli L R, Agarwal A and Dahotre N B 2000 *Mater. Sci. Eng.* A **289** 34
[23] Contreras A, León C A, Drew R A L and Bedolla E 2003 *Scr. Mater.* **48** 1625
[24] Aguilar E A, León C A, Contreras A, López V H, Drew R A L and Bedolla E 2002 *Composites* A **33** 1425
[25] Chun J S, Desjardins P, Petrov I, Greene J E, Lavoie C and Cabral C Jr 2001 *Thin Solid Films* **391** 69
[26] Ueshima M, Oku T, Inoue M, Tanihata K, Takahashi M and Suganuma K 1999 *Key Eng. Mater.* **161–163** 667
[27] Zhang F, Kaczmarek W A, Lu L and Lai M O 2000 *Scr. Mater.* **43** 109

[28] Ray A K, Venkateswarlu K, Chaudhury S K, Das S K, Kumar B R and Pathak L C 2002 *Mater. Sci. Eng.* A **338** 160
[29] Hansen L *et al Dacapo-1.30* Center for Atomic Scale Materials Physics (CAMP), Denmark Technical University
[30] Hohenberg P and Kohn W 1964 *Phys. Rev.* B **136** 864
[31] Kohn W and Sham L J 1965 *Phys. Rev.* A **140** 1133
[32] Vanderbilt D 1990 *Phys. Rev.* B **41** 7892
[33] Perdew J P, Chevary J A, Vosko S H, Jackson K A, Pederson M A, Singh D J and Fiolhais C 1992 *Phys. Rev.* B **46** 6671
[34] Kresse G and Forthmüller J 1995 *Comput. Mater. Sci.* **6** 15
[35] Neugebauer J and Scheffler M 1992 *Phys. Rev.* B **46** 16067
[36] Monkhorst H J and Pack J D 1976 *Phys. Rev.* B **13** 5188
[37] Murnaghan F D 1944 *Proc. Natl Acad. Sci. USA* **301** 2344
[38] Ahuja R, Eriksson O, Wills J M and Johansson B 1996 *Phys. Rev.* B **53** 3072
[39] Dunand A, Flack H D and Yvon K 1985 *Phys. Rev.* B **31** 2299
[40] Marlo M and Milman V 2000 *Phys. Rev.* B **62** 2899
[41] Schoenberg N 1954 *Acta Chem. Scand.* **8** 213
[42] Gubanov V A, Ivanovsky A L and Zhukov V P 1994 *Electronic Structure of Refractory Carbides and Nitrides* (Cambridge: Cambridge University Press)
[43] Hälglund J, Grimvall G, Jarlborg T and Guillermet A F 1991 *Phys. Rev.* B **43** 14400
[44] Asato M, Settlels A, Hoshino T, Asada T, Blügel S, Zeller R and Dederichs P H 1999 *Phys. Rev.* B **60** 5202
[45] Kittel C 1996 *Introduction to Solid State Physics* 7th edn (New York: Wiley)
[46] Boettger J C 1994 *Phys. Rev.* B **49** 16798
[47] Fiorentini V and Methfessel M 1996 *J. Phys.: Condens. Matter* **8** 6525
[48] Christensen A, Jarvis E A and Carter E A 2001 *Chemical Dynamic in Extreme Environment* ed R A Dreeler (Singapore: World Scientific) p 490
[49] Christensen A and Carter E A 2001 *J. Chem. Phys.* **114** 5816
[50] Rhee S K 1970 *J. Am. Ceram. Soc.* **53** 386
[51] Arya A and Carter E A 2003 *J. Chem. Phys.* **118** 8982
[52] Kobayashi K 2001 *Surf. Sci.* **493** 665
[53] Tagawa M, Kawasaki T, Oshima C, Otani S, Edamoto K and Nagashima A 2002 *Surf. Sci.* **517** 59
[54] Schnitker J and Srolovitz D J 1998 *Modelling Simul. Mater. Sci. Eng.* **6** 153
[55] Hong T, Smith J R and Srolovitz D J 1995 *Acta Metall. Mater.* **43** 2721
[56] Schnitker J and Srolovitz D J 1998 *Modelling Simul. Mater. Sci. Eng.* **6** 153
[57] Smith J R and Zhang W 2000 *Acta Mater.* **48** 4395
[58] Schönberger U, Andersen O K and Methfesse M 1992 *Acta Metall. Mater.* **40** S1